Title

Cerebrospinal fluid immune dysregulation during healthy brain aging and cognitive impairment.

Journal

Cell, 185(26)

Authors

Piehl, Natalie

van Olst, Lynn

Ramakrishnan, Abhirami

et al.

Publication Date

2022-12-22

DOI

10.1016/j.cell.2022.11.019

Peer reviewed

HHS Public Access

Author manuscript

Cell. Author manuscript; available in PMC 2023 December 22.

Published in final edited form as:

Cell. 2022 December 22; 185(26): 5028–5039.e13. doi:10.1016/j.cell.2022.11.019.

Cerebrospinal fluid immune dysregulation during healthy brain aging and cognitive impairment

Natalie Piehl[1], **Lynn van Olst**[1], **Abhirami Ramakrishnan**[1], **Victoria Teregulova**[1], **Brooke Simonton**[1], **Ziyang Zhang**[1], **Emma Tapp**[2], **Divya Channappa**[2], **Hamilton Oh**[3,4,5], **Patricia M. Losada**[2,3], **Jarod Rutledge**[3,4,6], **Alexandra N. Trelle**[7], **Elizabeth C. Mormino**[3,7], **Fanny Elahi**[8], **Douglas R. Galasko**[9], **Victor W. Henderson**[2], **Anthony D. Wagner**[3,7], **Tony Wyss-Coray**[2,3,4,10,11], **David Gate**[1,*]

[1]The Ken & Ruth Davee Department of Neurology, Northwestern University Feinberg School of Medicine, Chicago, IL, USA.

[2]Department of Neurology and Neurological Sciences, Stanford University School of Medicine, Stanford, California, USA.

[3]Wu Tsai Neurosciences Institute, Stanford University, Stanford, CA, USA.

[4]Paul F. Glenn Center for the Biology of Aging, Stanford University School of Medicine, Stanford, CA, USA.

[5]Graduate Program in Stem Cell and Regenerative Medicine, Stanford University, Stanford, CA, USA.

[6]Department of Genetics, Stanford University, Stanford, CA, USA.

[7]Department of Psychology, Stanford University, Stanford, CA, USA.

[8]Departments of Neurology and Neuroscience, Friedman Brain Institute, Icahn School of Medicine at Mount Sinai.

[9]Department of Neurosciences, University of California at San Diego, La Jolla, CA, USA.

[10]The Phil and Penny Initiative for Brain Resilience, Stanford University, Stanford, CA, USA.

[11]Chemistry, Engineering, and Medicine for Human Health (ChEM-H), Stanford University, Stanford, California, USA.

[*]Correspondence to: dgate@northwestern.edu.

Author Contributions

N.P. performed bioinformatics analysis and generated figures. L.v.O. directed experiments, edited figures and conducted confocal imaging. A.R., V.T., B.S., Z.Z., E.T. and D.C. assisted with sample processing. E.T. and D.G. performed cell sorting and library preparation. H.O., P.M.L. and J.L. assisted with CSF protein measurements and analysis. F.E., D.R.G., A.N.T., E.C.M., V.W.H. and A.D.W. provided patient samples. T.W-C. provided reagents. D.G. conceptualized and led the study and wrote the manuscript. All authors read and approved the final manuscript.

Declaration of Interests

T.W.-C. and D.G. are co-inventors on a patent related to this work. Patent US-2022-0170908-A1 is for compositions and methods for measuring T cell markers associated with Alzheimer's disease.

Abstract

Cerebrospinal fluid (CSF) contains a tightly regulated immune system. Yet, little is known about how CSF immunity is altered with aging or neurodegenerative disease. Here, we performed single cell RNA sequencing on CSF from 45 cognitively normal subjects ranging from 54–82 years old. We reveal upregulation of lipid transport genes in monocytes with age. We then compared this cohort to 14 cognitively impaired subjects. In cognitively impaired subjects, downregulation of lipid transport genes in monocytes occurred concomitantly with altered cytokine signaling to CD8 T cells. Clonal CD8 T effector memory cells upregulated *C-X-C Motif Chemokine Receptor 6* (*CXCR6*) in cognitively impaired subjects. The CXCR6 ligand, C-X-C Motif Chemokine Ligand 16 (CXCL16), was elevated in CSF of cognitively impaired subjects, suggesting CXCL16-CXCR6 signaling as a mechanism for antigen-specific T cell entry into the brain. Cumulatively, these results reveal cerebrospinal fluid immune dysregulation during healthy brain aging and cognitive impairment.

In brief

A single-cell transcriptomic resource exploring the cerebrospinal fluid immune system in healthy brain aging and disease uncovers the CXCL16-CXCR6 pathway as a mediator of $CD8^+$ T cell trafficking to the CSF.

Graphical Abstract

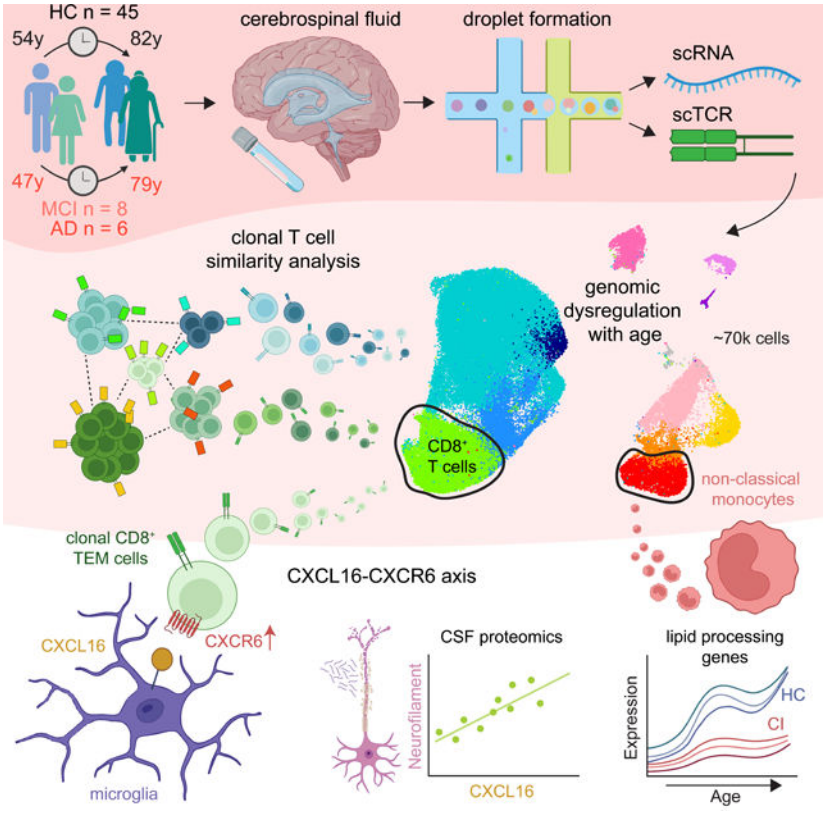

Neuroinflammation is a pathological hallmark of age-related neurodegenerative disease[1]. The brain is surrounded by the meninges, a membranous covering that contains the cerebrospinal fluid (CSF). The meningeal lymphatic system carries fluid and immune cells from the CSF to the deep cervical lymph nodes, enabling peripheral immune cells to respond to brain antigens under pathological conditions[2,3]. Adaptive immune T cells that initially encounter antigen in the periphery can enter the CSF via the systemic circulation and patrol the intrathecal space[4–7]. The choroid plexus, which produces the CSF, serves as an interface between the brain and circulation and is a site of age-related chronic neuroinflammation in mice[8,9]. Recent studies indicate the CSF provides molecular cues to immune cells of the skull bone marrow to alter CSF myeloid populations in mice[10–12]. Yet, the influence of age on the molecular mechanisms regulating CSF immunity in humans is not clear. Moreover, whether changes to the CSF immune system relate to behavioral changes such as cognitive impairment remains unknown.

Our recent studies indicate CSF immune changes reflect the pathobiological events of age-related neurodegenerative disorders such as Alzheimer's disease (AD)[13] and Lewy body dementia[14]. We thus hypothesized that comparing the CSF immune transcriptomes associated with healthy cognitive aging and cognitive impairment would provide insight into the pathophysiology of age-related neuroinflammation in neurodegenerative disease. Our results reveal age-related CSF immune perturbations in cognitively normal subjects, underscored by altered expression of lipid transport genes. Further, we detected upregulation of *C-X-C Motif Chemokine Receptor 6* (*CXCR6*) in clonally expanded $CD8^+$ T effector memory (T_{EM}) cells of cognitively impaired subjects. The CXCR6 ligand, C-X-C Motif Chemokine Ligand 16 (CXCL16) is a pleiotropic protein that functions as a T cell chemoattractant and scavenger receptor for oxidized lipoprotein. CXCL16 was elevated in CSF of cognitively impaired subjects and was associated with neuroaxonal damage. We localized $CXCR6^+$ T cells and $CXCL16^+$ myeloid cells to amyloid plaques in AD post-mortem brains. Therefore, our single cell transcriptomics resource identified the CXCL16-CXCR6 signaling axis as a potential mechanism for T cell entry into brains with neurodegeneration. Finally, we uncover an unexpected level of significantly altered AD risk genes in CSF T cells of cognitively impaired subjects. Altogether, these findings highlight the utility of measuring CSF immune changes to identify disease-associated neuroinflammation in cognitively impaired individuals.

Results

Assessing CSF immunity with age in healthy brain aging and cognitive impairment by scRNAseq

We first established age-related CSF immune transcriptome changes that occur with healthy brain aging. Extant studies on CSF immunity have suffered from biases associated with small sample sizes and limitations of conventional methods such as flow cytometry[15,16]. To circumvent these issues, we utilized our established droplet-based single cell RNA sequencing (scRNAseq) method[13,14,17] (Figure 1A). We generated CSF immune system profiles of 45 cognitively normal subjects ranging from 54–82 years old. We then compared CSF immune transcriptomes of this healthy cognitive aging group to 14 age- and sex-

matched patients with clinical diagnoses of AD or prodromal mild cognitive impairment (MCI) (Figure 1B and Supplemental Figure 1A–B). Comparison of Montreal Cognitive Assessment (MoCA) scores confirmed reduced cognitive abilities in MCI and AD subjects (Figure 1C). We also measured CSF biomarkers, which revealed higher levels of tau phosphorylated at residue 181 (pTau181) in cognitively impaired subjects (Figure 1C). Demographics and CSF biomarker data for these subjects are presented in Table 1.

Overall, we analyzed 70,391 quality-controlled CSF immune cells. Importantly, we did not observe diagnostic differences by dimensionality reduction (Supplemental Figure 1C). Further, quality control metrics indicated limited amounts of mitochondrial reads and expected numbers of counts and features per group (Supplemental Figure 1C). We then removed limited amounts of ambient RNA contamination with SoupX[18] (Supplemental Figure 1D–E). We resolved CSF immune cell types including $CD4^+$ and $CD8^+$ T cells, T regulatory cells (Tregs), natural killer (NK) cells, plasma cells, B cells, dendritic cells and three populations of classical, intermediate and non-classical monocytes distinguished by varying CD14 and CD16 expression and pseudotime analysis (Figure 1D and Supplemental Figure 1F). CSF immune clusters were annotated based on their expression of cardinal marker genes (Figure 1E). Number of counts and mitochondrial reads were also consistent per sample (Supplemental Figure 1G). We did not observe overt changes in cell type composition with age (Supplemental Figure 1H). Samples were processed on two separate days, but this did not introduce observable batch effects (Supplemental Figure 1I). We quantified cell type frequency, which revealed the majority of CSF immune cells as $CD4^+$ and $CD8^+$ T cells (Figure 1F). Finally, our full data set can be explored online using a data portal located at gatelabnu.shinyapps.io/csf_aging.

Linear CSF immune transcriptome changes associated with healthy brain aging

We began by assessing age-related transcriptomic changes to each cell type using linear regression. We noted that $CD4^+$ and $CD8^+$ T cells and non-classical monocytes had the most differentially expressed genes with age (Figure 1G and Supplemental Table 1). Plotting differentially expressed genes with age revealed increased expression of *Cluster of Differentiation 74* (*CD74*) among $CD4^+$ and $CD8^+$ T cells (Figure 1H). *CD74* encodes the human leukocyte antigen (HLA) class II histocompatibility antigen gamma chain, which is a marker of T cell activation[19–22]. $CD4^+$ and $CD8^+$ T cells also upregulated with age expression of genes encoding the granzyme family of serine proteases (Figure 1H and Supplemental Table 1). Granzymes are released by cytotoxic T cells to induce apoptosis in the target cell[23]. Interestingly, non-classical monocytes exhibited a pronounced reduction in expression with age of cytokine genes such as *C-C Motif Chemokine Ligand 3* (*CCL3*), *C-C Motif Chemokine Ligand 4 (CCL4*), *Tumor Necrosis Factor* (*TNF*) and *Interleukin 1 Beta* (*IL1B*). This reduction in cytokine gene expression was accompanied by increased expression of genes involved in lipid transport, including *Apolipoprotein E* (*APOE*), *Apolipoprotein C1* (*APOC1*) and *Phospholipid Transfer Protein* (*PLTP*) (Figure 1H). Notably, mutations in *APOE* and *APOC1* are associated risk factors for AD[24–30]. Further, the *PLTP* gene encodes a key determinant of lipoprotein metabolism involved in regulating inflammation, including by modulating adaptive immune functions through alternation of T cell polarization[31]. Thus, linear modeling revealed age-related changes

to the CSF immune system. These changes were underscored by altered expression of genes involved in lipoprotein metabolism that are also established genetic risk factors for age-related neurodegeneration.

Non-linear CSF immune transcriptome changes associated with healthy brain aging

When visualizing gene expression with age, we noted that CSF immune genes fluctuated in distinct, nonlinear patterns. We thus sought to visualize non-linear changes to CSF immune genes and to compare gene expression trajectories of CSF immune cells with age. Plotting expression of the 7,980 genes detected in nonclassical monocytes with age by locally estimated scatterplot smoothing (LOESS) revealed wave-like expression trajectories (Figure 2A). We used hierarchical clustering to identify distinct patterns of gene expression changes with age (Figure 2B, Supplemental Figure S2 and Supplemental Table 1). To further validate gene expression changes with age, we divided healthy control subjects into middle (<70 years) and advanced (≥70 years) age groups using the median age of 70 years old as a cut-off. We then performed differential expression by Model-based Analysis of Single Cell Transcriptomics (MAST)[32] (Figure 2C, Supplemental Figure 3B, and Supplemental Table 2). Importantly, we did not observe major effects of sex on the CSF immune transcriptome by MAST differential expression (Supplemental Figure 3A and Supplemental Table 2). Yet, differential expression of advanced and middle-aged groups also showed the highest level of immune dysregulation in non-classical monocytes (Figure 2C and Supplemental Table 2). We then plotted upregulated genes of non-classical monocytes by LOESS, which confirmed increased, non-linear expression of lipid transport genes *APOE*, *APOC1* and *PLTP* with age (Figure 2D). Thus, our non-linear analysis uncovered changes to lipid processing genes of nonclassical monocytes that dovetailed with our linear analysis.

We next sought to measure the age at which most gene expression changes were occurring. To measure non-linear gene expression changes, we used the algorithm Differential Expression - Sliding Window ANalysis (DE-SWAN)[33]. We used DE-SWAN to analyze gene levels within a window of four years by comparing groups in parcels of two years (e.g. 60–62y compared with 62–64y), while sliding the window in increments of two years from youngest to oldest (Figure 2E). Using DE-SWAN, we detected a peak of differential expression for several CSF immune clusters at age 78 (Figure 2F and Supplemental Table 3). Comparing differentially expressed genes by DE-SWAN and linear modeling underscored the effects of advanced age on non-classical monocytes (Figure 2G). We then plotted genes of each cluster by the significance of their differential expression at age 78, which revealed a large set of changing genes of Tregs and non-classical monocytes (Figure 2H, Supplemental Figure 3C and Supplemental Table 3). Notably, we detected dysregulated *Progranulin* (*GRN*) expression in nonclassical monocytes at age 78 (Figure 2H). Mutations in *GRN* are associated with AD[34] and frontotemporal dementia[35–37]. Intriguingly, *GRN* encodes a key regulator of lysosomal function[38] and lipid accumulation in brain microglia[39]. Lipid processing genes were also altered in non-classical monocytes at age 78, including *Apolipoprotein C2* and *Apolipoprotein B Receptor* (*APOBR*) (Figure 2H).

Activated monocytes communicate with CD8+ T cells via CXCL16-CXCR6 in cognitively impaired CSF

Having established gene expression patterns of CSF immune cells in healthy aging, we next aimed to compare these changes to subjects with cognitive impairment. To our surprise, MAST differential expression of cognitively impaired vs. cognitively normal controls revealed the highest level of transcriptomic dysregulation in Tregs (Supplemental Figure 4A and Supplemental Table 4). Analysis of individual differentially expressed genes showed upregulated expression of *Forkhead Box P3* (*FOXP3*) and *Interleukin 32* (*IL32*) in Tregs (Supplemental Figure 4B and Supplemental Table 4). Populations of classical and non-classical monocytes were also highly dysregulated (Supplemental Figure 4A). Interestingly, we noted downregulated expression of *APOC1* in non-classical monocytes (Supplemental Figure 4B). This prompted us to plot the expression of lipid processing genes of non-classical monocytes from cognitively impaired versus cognitively normal subjects with age. Plotting *APOE, APOC1* and *PLTP* with age by LOESS demonstrated reduced expression of all three genes in cognitively impaired subjects at later ages (Figure 2I). We thus performed MAST differential expression on non-classical monocytes comparing advanced age cognitively impaired subjects to advanced age cognitively normal subjects (Supplemental Figure 3D–E). By this method, *APOE* and *APOC1* were highly downregulated, verifying reduced expression of lipid processing genes in cognitively impaired subjects with age (Figure 2J and Supplemental Table 4).

We next aimed to determine whether reduced lipid processing gene expression among non-classical monocytes coincided with altered intercellular communication in the CSF. To infer cell-cell communication, we utilized CellChat. CellChat uses a signaling molecule interaction database of ligand-receptor interactions to analyze intercellular communications from scRNAseq data[40]. Within our scRNAseq data, cell-cell interactions of cognitively normal and cognitively impaired CSF appeared highly similar (Figure 3A). We detected the strongest incoming interactions among $CD8^+$ T cells and the strongest outgoing interactions coming from non-classical monocytes (Figure 3B). We then probed the cell-cell interactions of cognitively impaired CSF, which indicated strong communication probabilities between non-classical monocytes and $CD8^+$ T cells via human leukocyte antigen (HLA)-A, -B, -C and -E binding CD8A and CD8B (Figure 3C). In fact, most signaling pairs between non-classical monocytes and $CD8^+$ T cells that were increased in cognitively impaired CSF were also increased in cognitively normal CSF. Yet, signaling between C-X-C Motif Chemokine Ligand 16 (CXCL16) and C-X-C Motif Chemokine Receptor 6 (CXCR6) was unique to cognitively impaired CSF (Figure 3D). Notably, CXCR6 is a surface chemokine receptor that regulates T cell migration to various tissues[41]. We then plotted the cell-cell interactions of CXCL16-CXCR6 signaling in cognitively impaired CSF, which indicated non-classical monocytes as the primary source of CXCL16 for CXCR6 expressed on $CD8^+$ T cells (Figure 3E). We measured *CXCL16* and *CXCR6* among CSF cell types, which indicated expression of *CXCL16* by myeloid cells and *CXCR6* by T cells (Figure 3F–G). We next sequenced CSF T cell receptors (TCRs) from the same cells as above and noted an association of *CXCR6* expression with clonal T cells (Figure 3H). Altogether, these results show that myeloid cells communicate with $CD8^+$ T cells via CXCL16-CXCR6 in cognitively impaired

CSF. Interestingly, we also detected clonally expanded Tregs (Supplemental Figure S4C), but these cells were too sparse to perform differential expression.

Dysregulation of clonally expanded CSF T cells of cognitively impaired subjects

We previously showed that clonally expanded T cells patrol the CSF in AD[14]. However, the mechanism by which antigen-specific T cells enter the CSF remains poorly understood. We therefore assessed the transcriptomes of clonally expanded T cells between cognitively impaired vs. cognitively normal CSF immune systems. We then asked whether CSF TCRs from cognitively impaired subjects were similar in protein sequence to those of cognitively normal subjects of advanced age. We used our established TCR Levenshtein similarity networking method[13,17,42] to compare TCRs of cognitively impaired patients to cognitively normal subjects of four equal sized age bins (early and late middle age and early and late advanced age). These results showed increased similarity of TCRs from cognitively impaired subjects with the two oldest age bins (early and late advanced age) (Figure 4A and Supplemental Table 4). Conversely, no similarities were detected between TCRs from cognitively impaired subjects with the two youngest age bins (Figure 4A–B and Supplemental Table 4).

We next sought to determine whether clonally expanded, antigen-specific T cells were transcriptionally distinct in cognitively impaired vs. cognitively normal CSF immune systems. We thus performed differential expression on clonally expanded $CD4^+$ and $CD8^+$ T cells of cognitively impaired vs. cognitively normal CSF. MAST differential expression of non-clonal and clonal $CD4^+$ and $CD8^+$ T cells revealed T cell clonal expansion as a driver of transcriptional dysregulation in cognitively impaired vs. cognitively normal CSF (Figure 4C). We noted a shift from *CXCR4* to *CXCR6* chemokine receptor gene expression in clonally expanded $CD4^+$ and $CD8^+$ T cells (Supplemental Figure 5A–B). Notably, clonally expanded $CD8^+$ T cells upregulated *CXCR6* in cognitively impaired vs. cognitively normal CSF (Figure 4D and Supplemental Table 4). We further confirmed increased *CXCR6* expression by $CD8^+$ T cells in cognitively impaired subjects on the pseudobulk level (Supplemental Figure 5C).

We next aimed to obtain finer resolution of the $CD8^+$ T cell subtype associated with cognitive impairment. To do so, we utilized a Cellular Indexing of Transcriptomes and Epitopes by Sequencing (CITE-seq) reference dataset[43] and supervised clustering to reannotate the same CSF cells (Supplemental Figure 5D–E). To our surprise, $CD14^+$ monocytes were the most dysregulated cell type among reannotated clusters (Supplemental Figure 5F and Supplemental Table 5). Having finer resolution of CSF immunity, we then measured *CXCR6* expression in T cell subsets, which distinguished $CD8^+$ and $CD4^+$ T_{EM} cells as the primary expressors of *CXCR6* (Figure 4F and Supplemental Figure 5G). We also observed increased *CXCR6* expression in $CD8^+$ T_{EM} cells on the pseudobulk level (Supplemental Figure 5H). We then reassigned TCRs to these reannotated cells to identify clonal populations of CSF T cells (Figure 4G and Supplemental Figure 5I). We quantified single cell expression of *CXCR6* on CD8 T_{EM} cells which revealed higher levels of expression among cognitively impaired subjects (Figure 4H).

Finally, we sought to measure levels of CSF CXCL16 protein in larger groups of subjects and to compare CXCL16 levels to neurodegenerative disease biomarkers. We first utilized a proximity extension assay (PEA), which detected higher levels of CXCL16 in CSF of cognitively impaired vs. cognitively normal subjects (Figure 4I and Supplemental Figure 6A). Notably, levels of CXCL16 highly correlated with levels of neurofilament light (NEFL) in cognitively impaired and cognitively normal subjects (Figure 4J and Supplemental Table 6). NEFL is a biomarker for neuroaxonal damage which predicts neurodegeneration and clinical progression in presymptomatic AD[44]. CXCL16 also correlated with levels of CSF glial fibrillary acidic protein (GFAP) and ubiquitin C-terminal hydrolase L1 (UCHL1). Interestingly, CXCL16 did not correlate with either $A\beta_{40}$ or $A\beta_{42}$, but did correlate with pTau181 in subjects who were diagnosed with MCI and progressed to AD (Figure 4J). We confirmed our PEA results by detecting a positive correlation between CXCL16 and NEFL by slow off-rate modified aptamer (SOMAmer) assay (Figure 4K and Supplemental Table 6). However, although the SOMAmer assay detected increased levels of CXCL16 in cognitively impaired subjects, we did not observe significant group differences (Supplemental Figure 6B).

Interestingly, public datasets indicate that microglia/macrophages are the main expressors of *CXCL16* in human brain (Supplemental Figure 6C)[45]. Further, microglia express higher levels of *CXCL16* than monocytes (Supplemental Figure 6D)[46]. In AD brain, *CXCL16* is more highly expressed in the temporal cortex of AD subjects than controls (Supplemental Figure 6E)[47]. Thus, we aimed to confirm protein expression of CXCL16 in AD brain myeloid cells. Indeed, we identified $CXCL16^{+}Iba1^{+}$ plaque-associated myeloid cells in AD brain (Supplemental Figure 6F). We confirmed intracellular expression of CXCL16 by $Iba1^{+}$ cells by generating a z-stack through an $Iba1^{+}$ myeloid cell body (Supplemental Figure 6G). Finally, we identified $CD3^{+}$ T cells expressing the CXCR6 receptor in close proximity to $Iba1^{+}$ myeloid cells in two separate AD post-mortem brains (Supplemental Figure 6H). Cumulatively, these results indicate altered CXCR6-CXCL16 signaling as a mechanism for antigenexperienced T cell entry into the brains of subjects with neurodegeneration.

Our results uncover T cell transcriptomic changes associated with cognitive impairment. Historically, innate immunity has been studied in greater detail than adaptive immunity in AD. The identification of AD risk genes via genome wide association studies (GWAS)[48,49] further compelled AD researchers to interrogate brain innate immunity, since many AD risk genes are expressed by brain innate immune cells. Yet, when we probed AD risk genes for expression among CSF immune cells[50], we identified $CD4^{+}$ and $CD8^{+}$ T cells as having the most significantly altered genes (Figure 5). Among supervised clusters, $CD4^{+}$ T_{EM} and $CD8^{+}$ T_{EM} cells had the most differentially expressed AD risk genes (Supplemental Figure 6I). Altogether, these results uncover a potential, unexpected role of T cells in AD risk.

Discussion

Our CSF immune transcriptomic profiling provides insight into the influence of age on healthy brain aging and into the pathophysiology of cognitive impairment. In healthy brain aging, we identified a population of non-classical CSF monocytes with increased expression of genes encoding lipid processing proteins. Some of the genes associated with CSF

monocyte aging are genetic risk factors for AD, including *APOE* and *APOC1*. Increased expression of these genes by intrathecal monocytes highlights the critical role of lipid metabolism in innate immunity and immunoregulation[51]. Particularly intriguing was the concomitant downregulation of cytokine genes, suggestive of a metabolic and functional shift of non-classical monocytes with age. These changes might reflect parenchymal myeloid cell pathophysiology, such as the accumulation of lipid droplets in brain microglia with age[39].

Our results also indicate disparate age-related CSF immune system perturbations in cognitively impaired subjects. These transcriptional changes may reflect alterations to CSF immunity during the neurodegenerative disease course. Among significantly altered CSF immune cells were non-classical monocytes, which show decreased expression of lipid transport genes concomitant with increased signaling to $CD8^+$ T cells via CXCL16-CXCR6. Intriguingly, CXCL16 has a dual role as a scavenger receptor that mediates internalization of oxidized low-density lipoproteins[52]. Thus, increased CXCL16 in the CSF of cognitively impaired subjects may be compensatory to reduced lipid transport gene expression in non-classical monocytes. Additionally, CXCL16 is a receptor for phosphatidylserine-coated particles such as apoptotic bodies. Therefore, the correlation between CXLC16 and neuroaxonal damage may reflect the immune response to neuronal death.

Our results show that TCRs of cognitively impaired subjects more closely resemble those from advanced ages than younger age groups. This suggests that the TCR repertoire of cognitively impaired subjects resembles an “advanced aging” CSF adaptive immune system. Moreover, we identify an association of *CXCR6* expression in clonally expanded T cells and cognitive impairment. Our results suggest that CXCR6 regulates homing of antigen-specific T cells from the peripheral circulation to the CSF via brain myeloid expression of CXCL16. This finding is particularly enlightening in conjunction with recent evidence that CXCR6/CXCL16 signaling functions as a maintenance factor for brain resident T cells that drive synapse elimination during viral recovery in mice[53].

Altogether, our results highlight the potential to utilize CSF immune transcriptome changes to identify disease-associated neuroinflammation in cognitively impaired individuals. As such, CSF immunophenotyping may be useful to gain further insight into T cell-antigen complexes involved in the pathophysiology of cognitive impairment. Here, we uncover CXCL16-CXCR6 signaling as a potential mechanism of antigen-specific T cell entry into the intrathecal space of patients with cognitive impairment. These findings could be used to improve anti-inflammatory therapeutics or to estimate levels of neuroinflammation in cognitively impaired patients.

Limitations of the Study

This study is comprised entirely of human data and our claims are based primarily on bioinformatic approaches that rely on underlying assumptions of algorithms. As such, there are limitations regarding functional or mechanistic evidence. Ideally, in vivo experiments in animals would further elucidate the necessity and sufficiency of CXCL16-CXCR6 signaling in T cell brain homing and its impact on cognition. We encourage animal researchers to interrogate this pathway. Additionally, females comprised most of the younger healthy

controls, while males comprised most of the older healthy controls in this study. Thus, we suggest further interrogation of potential sex differences in CSF immunity.

STAR Methods

RESOURCE AVAILABILITY

Lead Contact—Further information and requests for resources should be directed to and will be fulfilled by the lead contact, David Gate (dgate@northwestern.edu).

Materials Availability—No new unique reagents were generated for this study.

Data and Code Availability

- All raw data used in this study can be found on GEO with accession number GEO200164. Raw count and log-normalized expression matrices are also available under the same accession number.
- All code used to generate the figures in this study can be found at https://github.com/gatelabnw/csf_aging.
- Any additional information required to reanalyze the data reported in this work paper is available from the Lead Contact upon request.

EXPERIMENTAL MODEL AND SUBJECT DETAILS

Human Subjects—For scRNAseq experiments, CSF samples were acquired through the Stanford Aging and Memory Study (SAMS), Stanford University Alzheimer's Disease Research Center (ADRC), the University of California at San Francisco ADRC and the University of California at San Diego ADRC. Collection of CSF was approved by the Institutional Review Board of each university and written consent was obtained from all subjects. scRNAseq and scTCRseq were performed on CSF of 59 subjects of both sexes aged 47–82 years. Of these subjects, 45 were assessed as healthy controls while the remaining 14 were patients with cognitive impairment (MCI or dementia due to AD). Age and sex demographics are presented in Supplemental Figure 1A–B. SAMS eligibility included normal or corrected to-normal vision/hearing, native English speaking, no history of neurologic or psychiatric disease, a Clinical Dementia Rating (CDR) global score of zero, and performance within the normal range on a standardized neuropsychological test battery[54,55]. In the ADRCs, all healthy control participants had CDR scores of zero and were deemed cognitively unimpaired during a clinical consensus meeting consisting of neurologists, neuropsychologists, and research coordinators. All healthy control and cognitively impaired study subjects underwent neurological examinations, CDR ratings, and standardized neuropsychological assessments to determine cognitive and diagnostic status, including procedures of the National Alzheimer's Coordinating Center. All cognitively impaired participants had a CDR score greater than zero. For histology experiments, de-identified human dorsolateral prefrontal cortex samples from AD subjects of various ages were obtained through collaboration with the Stanford University ADRC.

METHOD DETAILS

Sample Preparation—CSF was collected via lumbar puncture and cells were cryopreserved according to our established protocol[17]. All 59 CSF samples were processed and cryopreserved by the same technician over the course of two years. Cells were sorted by FACS for live singlets using Sytox blue live/dead dye before performing droplet-based scRNAseq and scTCRseq.

Protein biomarker measurements—We measured protein biomarkers in CSF with two separate methods. We used PEA technology (Olink Proteomics) to measure CXCL16 and NEFL as in Figure 4I–J. Protein levels are presented in Normalized Protein eXpression (NPX) units. NPX is Olink's arbitrary unit, which is in Log2 scale. NPX is calculated from Ct values and data pre-processing (normalization) is performed to minimize both intra- and inter-assay variation. Separately, we used single molecule array (Simoa) ELISA technology (Quanterix) to measure NEFL, $A\beta_{42}$ and $A\beta_{40}$, as in Figure 4J. We also measured CXCL16 and NEFL using SOMAmer technology (SomaLogic), as in Figure 4K.

Droplet-based scRNA and TCRseq—The 10x Genomics Chromium Next GEM Single Cell 5' v2 with immune profiling kit was used for scRNA and TCRseq of CSF samples. Libraries were prepared according to 10x Genomics protocols. Libraries were sequenced by Novogene on an Illumina Novaseq 6000 instrument. Bases were called using the Illumina RTA3 method. RNA reads were aligned to the hg38 genome build and gene expression matrices were generated using Cell Ranger 6.0.0 software. TCR reads were also aligned to the hg38 genome build and clonotype/contig matrices were generated using Cell Ranger.

scRNA and TCRseq quality control—Empty droplets were removed via Cell Ranger 6.0.0 using the EmptyDrops method per 10x Genomics' protocol. Gene expression matrices were corrected for background contamination using R package SoupX 1.5.2. Known monocyte/dendritic markers (CD14, CD68, MS4A7, and CD16) were used to estimate the contamination fraction of each sample. Counts were adjusted using the SoupX subtraction method using the calculated contamination fraction on a per sample basis. Doublets were removed using R package DoubletFinder 2.0.3[56] using an approximate doublet formation rate of 1% which is consistent with the expected multiplet rate according to 10x Genomics Single Cell 5' v2 kit protocol. Any cells with fewer than 200 mapped features were eliminated, as well as any features present in fewer than three cells. Any cells with greater than 10% mitochondrial reads were also eliminated. TCR clonotypes and contigs were also filtered for empty droplets using Cell Ranger 6.0.0. Only TCR sequences associated to cells annotated with a T cell identity by RNAseq were retained.

Cell type annotations—Corrected and filtered gene expression matrices were SCTransformed with Seurat 4.1.0[43] on a per sample basis and then integrated through harmonizing 'anchors' as recommended for cell type identification in Seurat documentation. Number of reads, number of features, and percent of mitochondrial reads were regressed out in the data scaling step of SCTransform, and the top 1000 most variable features were used. Principal component analysis (PCA) was then run on the integrated assay. The first fifteen principal components (PCs) were then used to generate a shared nearest neighbor graph

which was then clustered under the Louvain algorithm with a resolution of 0.3. Uniform manifold approximation and projection (UMAP) was then performed using the first 15 PCs and 30 nearest neighbors. Canonical cell type markers were used to identify expected cell types (markers used are shown in Fig.1D). Pan T cell and monocyte clusters were then isolated, and the clustering procedure was repeated to differentiate more specific cell types.

Differential expression by linear modelling—We first aimed to identify genes with linear expression changes across age. The following model was implemented:

$$Expression \sim \alpha + \beta_1\, age + \beta_2\, sex + \varepsilon$$

Log-normalized counts were used for expression values as recommended for differential expression analyses by the developers of Seurat. α represents the y-intercept, β values represent the associated slope with the variable of interest, and ε represents residual error. Sex was included as a covariate to account for variations in sex composition of the cohort across age. Only genes expressed in at least 10% of cells in the respective cell type were used for differential expression throughout the study. Linear models were generated using the R package stats function, *lm*. Type II sum of squares were calculated using the R package car function, *Anova.* P values were adjusted for multiple comparisons using the Benjamini-Hochberg procedure. Thresholds of 0.01 for adjusted p value and 0.005 for β were used to determine significant DEGs.

DE-SWAN analysis—DE-SWAN was implemented to identify more transient gene expression changes across age. The following model was used:

$$Expression \sim \alpha + \beta_1 I_{k\ low/high} + \varepsilon$$

$I_{k\ low/high}$ represents the binarization of age binned above and below k centers. 10 centers with windows of ± 2 years from ages 62 to 82 were used. Number of cells per age bin per cell type differed dramatically from one center to the next. To mitigate the effect of cell number on number of DEGs, we randomly sampled 200 cells with replacement from each age for each cell type. Gene counts for every twenty cells were summed to generate a ‘pseudocell’ and then log-normalized. Type II sum of squares were calculated using the R package car function, *Anova.* P values were adjusted for multiple comparisons using the Benjamini-Hochberg procedure. Significant DEGs were identified with thresholds of 1e-4 for adjusted p value and 1e-4 for β.

LOESS trajectory analysis—LOESS was employed to identify non-linear patterns of gene expression over age. We initially focused on healthy aging and thus selected cognitively normal samples only. To avoid variable cell number per sample skewing the analysis, we proceeded with pseudobulked expression values. Counts for each cell type per sample were summed and then log-normalized. Genes were filtered for expression by at least 10% of cells per cell type and expression values were scaled and centered. A LOESS regression of span 0.75 was fit to each gene using the *loess* function of the R stats package. The predicted expression trajectories over age were then subdivided into 6 and 12 groups by

hierarchal clustering via *hclust* function from the R stats package. LOESS curves of average expression per age point in each cluster are also reported with their associated standard errors.

Differential expression by MAST—The Seurat function *FindMarkers* was used to identify DEGs across age and diagnosis. MAST was chosen to test significance as it employs a hurdle model specifically tailored to bimodal expression distributions often observed in scRNAseq. Only genes expressed in at least 10% of cells were tested. Sex was included as a latent variable to account for sex composition changes in the cohort across age. P values were adjusted for multiple comparisons using the Benjamini-Hochberg procedure. Genes with an adjusted p value less than 0.01 and average log-fold change magnitude greater than 0.25 were considered significantly differentially expressed.

CellChat analysis—The R package CellChat[40] was used to quantitatively infer and analyze intercellular communication networks from our scRNAseq data. CellChat uses network analysis and pattern recognition approaches to predict major signaling inputs and outputs for cells and how those cells and signals coordinate for functions. CellChat classifies signaling pathways and delineates conserved and context-specific pathways through manifold learning and quantitative contrasts. CellChat calculates the communication probability of a ligand-receptor pair between two cell types using a law of mass action model which depends on ligand and receptor concentration, any known cofactor concentrations, and the number of cells in each cell type. Significance is determined by if this communication probability is statistically higher between these known cell types than between randomly permuted groups of cells.

Levenshtein similarity network—Clonotypes with unambiguous CDR3 regions on both α and β chains and a frequency of at least 2 were retained to assess TCR similarity. Both CDR3 regions were concatenated together for each cell and Levenshtein similarity (Lsim)[42] was calculated between every possible TCR pair within and between all samples. Lsim was calculated by first finding the minimum number of deletions, additions, or substitutions needed to change one string to another, this value being the Levenshtein distance. This distance was then divided by the maximum length of both strings and subtracted from 1 to generate the Lsim. Individuals were binned into four healthy, cognitively normal age groups of equal size and one cognitively impaired group. TCR pairs with an Lsim of at least 0.9 were used for visualization on the network plot.

Clone expression scatterplot—We aimed to evaluate the heterogeneity of gene expression in cells of expanded or individual T cell clones in healthy versus cognitively impaired individuals. The top five most expanded clones in healthy and diseased individuals were selected. To create nonclonal bootstrap cells, fifty clones of frequency 1 were randomly selected from each diagnosis group. These 50 cells were sequestered into 5 groups and gene counts were summed then log-normalized. Average expression of all cells within an expanded clone as well as the percentage of cells in a clone/bootstrap expressing the gene of interest were calculated.

Immunohistochemistry and confocal imaging—We stained 5μm paraffin embedded brain tissue sections using antibodies rat anti-CD3 (Abcam ab11089), rabbit anti-CXCR6 (Abcam ab273116), mouse anti-CXCL16 (Thermo MA5–27845), rabbit anti-amyloid-β (Cell Signaling 8243) and goat anti-Iba1 (Abcam ab48004). Sections were deparaffinized, then antigen retrieval was performed using citrate buffer pH 6.0 for 30 min at 95°C. Sections were blocked in phosphate buffered saline containing 10% normal donkey serum and 0.1% triton-x. Sections were stained overnight in primary antibodies. The following morning, sections were incubated with highly cross-absorbed, species-appropriate secondary antibodies. Sections were imaged on a Nikon AXR confocal microscope with a 60x objective.

ShinyCell—ShinyCell is an R package developed to quickly generate interactive Shiny-based web applications to visualize the core analysis of scRNAseq data. We have released a modified ShinyCell app allowing users to view metadata and gene expression on a UMAP, compare gene expression between various groups via violin/box plots, and other built-in analyses. Notably, we added an additional page allowing the user to view LOESS trajectories of any gene of interest between HC and CI patients in a selected cell type as well as download the associated pseudobulk data.

QUANTIFICATION AND STATISTICAL ANALYSIS

R 4.1.1 and Prism 9.2.0 were used for all statistical analyses. Statistical methods are described in the figure legends or main text as appropriate.

Supplementary Material

Refer to Web version on PubMed Central for supplementary material.

Acknowledgements

We thank A.C. Yang (UC San Francisco) and R.T. Vest (Qinotto Inc.) for helpful advice. We also thank the clinical staffs of the Stanford Alzheimer's Disease Research Center (ADRC) and the Stanford Brain Rejuvenation Program for their assistance acquiring patient samples. Some figures were created using BioRender.com. This work was supported by a NIA R01AG078713-01 (D.G.), a 10x Genomics Early Career Investigator Award (D.G.), a National Institute of Neurologic Disease and Stroke K99/R00 Pathway to Independence Award NS112458-01A1 (D.G.), an Irene Diamond Fund/AFAR Postdoctoral Transition Award in Aging (D.G.), the Cure Alzheimer's Fund (D.G.), the Alzheimer's Association ADSF-21-818117 (D.G. and T.W-C.), the NOMIS Foundation (T.W-C.), NIA R01AG045034 05 (T.W-C.), the NIA funded Stanford ADRC P50AG047366 and P30AG066515 (V.W.H.), R01AG048076 (A.D.W), UC San Diego Shiley-Marcos ADRC P30 AG062429 (D.R.G.), and a pilot project through the Northwestern University ADRC 1P30AG072977-01 (D.G.).

References

1. Wyss-Coray T, and Mucke L. (2002). Inflammation in neurodegenerative disease--a double-edged sword. Neuron 35, 419–432. 10.1016/s0896-6273(02)00794-8. [PubMed: 12165466]
2. Aspelund A, Antila S, Proulx ST, Karlsen TV, Karaman S, Detmar M, Wiig H, and Alitalo K. (2015). A dural lymphatic vascular system that drains brain interstitial fluid and macromolecules. J Exp Med 212, 991–999. 10.1084/jem.20142290. [PubMed: 26077718]
3. Louveau A, Smirnov I, Keyes TJ, Eccles JD, Rouhani SJ, Peske JD, Derecki NC, Castle D, Mandell JW, Lee KS, et al. (2015). Structural and functional features of central nervous system lymphatic vessels. Nature 523, 337–341. 10.1038/nature14432. [PubMed: 26030524]

4. Bartholomaus I, Kawakami N, Odoardi F, Schlager C, Miljkovic D, Ellwart JW, Klinkert WE, Flugel-Koch C, Issekutz TB, Wekerle H, and Flugel A. (2009). Effector T cell interactions with meningeal vascular structures in nascent autoimmune CNS lesions. Nature 462, 94–98. 10.1038/nature08478. [PubMed: 19829296]
5. Kivisakk P, Mahad DJ, Callahan MK, Trebst C, Tucky B, Wei T, Wu L, Baekkevold ES, Lassmann H, Staugaitis SM, et al. (2003). Human cerebrospinal fluid central memory CD4+ T cells: evidence for trafficking through choroid plexus and meninges via P-selectin. Proc Natl Acad Sci U S A 100, 8389–8394. 10.1073/pnas.1433000100. [PubMed: 12829791]
6. Reboldi A, Coisne C, Baumjohann D, Benvenuto F, Bottinelli D, Lira S, Uccelli A, Lanzavecchia A, Engelhardt B, and Sallusto F. (2009). C-C chemokine receptor 6-regulated entry of TH-17 cells into the CNS through the choroid plexus is required for the initiation of EAE. Nat Immunol 10, 514–523. 10.1038/ni.1716. [PubMed: 19305396]
7. Schlager C., Korner H., Krueger M., Vidoli S., Haberl M., Mielke D., Brylla E., Issekutz T., Cabanas C., Nelson PJ., et al. . (2016). Effector T-cell trafficking between the leptomeninges and the cerebrospinal fluid. Nature 530, 349–353. 10.1038/nature16939. [PubMed: 26863192]
8. Baruch K, Deczkowska A, David E, Castellano JM, Miller O, Kertser A, Berkutzki T, BarnettItzhaki Z, Bezalel D, Wyss-Coray T, et al. (2014). Aging. Aging-induced type I interferon response at the choroid plexus negatively affects brain function. Science 346, 89–93. 10.1126/science.1252945. [PubMed: 25147279]
9. Schwartz M. (2017). Can immunotherapy treat neurodegeneration? Science 357, 254–255. 10.1126/science.aai8231. [PubMed: 28729500]
10. Cugurra A, Mamuladze T, Rustenhoven J, Dykstra T, Beroshvili G, Greenberg ZJ, Baker W, Papadopoulos Z, Drieu A, Blackburn S, et al. (2021). Skull and vertebral bone marrow are myeloid cell reservoirs for the meninges and CNS parenchyma. Science 373. 10.1126/science.abf7844.
11. Mazzitelli JA, Smyth LCD, Cross KA, Dykstra T, Sun J, Du S, Mamuladze T, Smirnov I, Rustenhoven J, and Kipnis J. (2022). Cerebrospinal fluid regulates skull bone marrow niches via direct access through dural channels. Nat Neurosci 25, 555–560. 10.1038/s41593-022-01029-1. [PubMed: 35301477]
12. Pulous FE, Cruz-Hernandez JC, Yang C, Kaya Z, Paccalet A, Wojtkiewicz G, Capen D, Brown D, Wu JW, Schloss MJ, et al. (2022). Cerebrospinal fluid can exit into the skull bone marrow and instruct cranial hematopoiesis in mice with bacterial meningitis. Nat Neurosci 25, 567–576. 10.1038/s41593-022-01060-2. [PubMed: 35501382]
13. Gate D, Saligrama N, Leventhal O, Yang AC, Unger MS, Middeldorp J, Chen K, Lehallier B, Channappa D, De Los Santos MB, et al. (2020). Clonally expanded CD8 T cells patrol the cerebrospinal fluid in Alzheimer's disease. Nature 577, 399–404. 10.1038/s41586-019-1895-7. [PubMed: 31915375]
14. Gate D, Tapp E, Leventhal O, Shahid M, Nonninger TJ, Yang AC, Strempfl K, Unger MS, Fehlmann T, Oh H, et al. (2021). CD4(+) T cells contribute to neurodegeneration in Lewy body dementia. Science 374, 868–874. 10.1126/science.abf7266. [PubMed: 34648304]
15. Kowarik MC, Grummel V, Wemlinger S, Buck D, Weber MS, Berthele A, and Hemmer B. (2014). Immune cell subtyping in the cerebrospinal fluid of patients with neurological diseases. J Neurol 261, 130–143. 10.1007/s00415-013-7145-2. [PubMed: 24162037]
16. Svenningsson A., Hansson GK., Andersen O., Andersson R., Patarroyo M., and Stemme S. (1993). Adhesion molecule expression on cerebrospinal fluid T lymphocytes: evidence for common recruitment mechanisms in multiple sclerosis, aseptic meningitis, and normal controls. Ann Neurol 34, 155–161. 10.1002/ana.410340210. [PubMed: 8338339]
17. Oh H, Leventhal O, Channappa D, Henderson VW, Wyss-Coray T, Lehallier B, and Gate D. (2021). Methods to investigate intrathecal adaptive immunity in neurodegeneration. Mol Neurodegener 16, 3. 10.1186/s13024-021-00423-w. [PubMed: 33482851]
18. Young MD, and Behjati S. (2020). SoupX removes ambient RNA contamination from droplet-based single-cell RNA sequencing data. Gigascience 9. 10.1093/gigascience/giaa151.
19. Baecher-Allan C, Wolf E, and Hafler DA (2006). MHC class II expression identifies functionally distinct human regulatory T cells. J Immunol 176, 4622–4631. 10.4049/jimmunol.176.8.4622. [PubMed: 16585553]

20. Saraiva DP, Jacinto A, Borralho P, Braga S, and Cabral MG (2018). HLA-DR in Cytotoxic T Lymphocytes Predicts Breast Cancer Patients' Response to Neoadjuvant Chemotherapy. Front Immunol 9, 2605. 10.3389/fimmu.2018.02605. [PubMed: 30555458]
21. Tippalagama R, Singhania A, Dubelko P, Lindestam Arlehamn CS, Crinklaw A, Pomaznoy M, Seumois G, deSilva AD, Premawansa S, Vidanagama D, et al. (2021). HLA-DR Marks Recently Divided Antigen-Specific Effector CD4 T Cells in Active Tuberculosis Patients. J Immunol 207, 523–533. 10.4049/jimmunol.2100011. [PubMed: 34193602]
22. Viallard JF, Bloch-Michel C, Neau-Cransac M, Taupin JL, Garrigue S, Miossec V, Mercie P, Pellegrin JL, and Moreau JF (2001). HLA-DR expression on lymphocyte subsets as a marker of disease activity in patients with systemic lupus erythematosus. Clin Exp Immunol 125, 485–491. 10.1046/j.1365-2249.2001.01623.x. [PubMed: 11531958]
23. Peters PJ, Borst J, Oorschot V, Fukuda M, Krahenbuhl O, Tschopp J, Slot JW, and Geuze HJ (1991). Cytotoxic T lymphocyte granules are secretory lysosomes, containing both perforin and granzymes. J Exp Med 173, 1099–1109. 10.1084/jem.173.5.1099. [PubMed: 2022921]
24. Bertram L, McQueen MB, Mullin K, Blacker D, and Tanzi RE (2007). Systematic meta-analyses of Alzheimer disease genetic association studies: the AlzGene database. Nat Genet 39, 17–23. 10.1038/ng1934. [PubMed: 17192785]
25. Chartier-Harlin MC., Parfitt M., Legrain S., Perez-Tur J., Brousseau T., Evans A., Berr C., Vidal O., Roques P., Gourlet V., and et al. . (1994). Apolipoprotein E, epsilon 4 allele as a major risk factor for sporadic early and late-onset forms of Alzheimer's disease: analysis of the 19q13.2 chromosomal region. Hum Mol Genet 3, 569–574. 10.1093/hmg/3.4.569. [PubMed: 8069300]
26. Drigalenko E, Poduslo S, and Elston R. (1998). Interaction of the apolipoprotein E and CI loci in predisposing to late-onset Alzheimer's disease. Neurology 51, 131–135. 10.1212/wnl.51.1.131. [PubMed: 9674791]
27. Farrer LA, Cupples LA, Haines JL, Hyman B, Kukull WA, Mayeux R, Myers RH, Pericak-Vance MA, Risch N, and van Duijn CM (1997). Effects of age, sex, and ethnicity on the association between apolipoprotein E genotype and Alzheimer disease. A meta-analysis. APOE and Alzheimer Disease Meta Analysis Consortium. JAMA 278, 1349–1356. [PubMed: 9343467]
28. Ki CS, Na DL, Kim DK, Kim HJ, and Kim JW (2002). Genetic association of an apolipoprotein C-I (APOC1) gene polymorphism with late-onset Alzheimer's disease. Neurosci Lett 319, 75–78. 10.1016/s0304-3940(01)02559-9. [PubMed: 11825674]
29. Kuerban B, Shibata N, Komatsu M, Ohnuma T, and Arai H. (2010). Genetic association between PLTP gene polymorphisms and Alzheimer's disease in a Japanese population. Dement Geriatr Cogn Disord 30, 78–82. 10.1159/000318855. [PubMed: 20714154]
30. Tycko B, Lee JH, Ciappa A, Saxena A, Li CM, Feng L, Arriaga A, Stern Y, Lantigua R, Shachter N, and Mayeux R. (2004). APOE and APOC1 promoter polymorphisms and the risk of Alzheimer disease in African American and Caribbean Hispanic individuals. Arch Neurol 61, 1434–1439. 10.1001/archneur.61.9.1434. [PubMed: 15364690]
31. Desrumaux C, Lemaire-Ewing S, Ogier N, Yessoufou A, Hammann A, Sequeira-Le Grand A, Deckert V, Pais de Barros JP, Le Guern N, Guy J, et al. (2016). Plasma phospholipid transfer protein (PLTP) modulates adaptive immune functions through alternation of T helper cell polarization. Cell Mol Immunol 13, 795–804. 10.1038/cmi.2015.75. [PubMed: 26320740]
32. Finak G, McDavid A, Yajima M, Deng J, Gersuk V, Shalek AK, Slichter CK, Miller HW, McElrath MJ, Prlic M, et al. (2015). MAST: a flexible statistical framework for assessing transcriptional changes and characterizing heterogeneity in single-cell RNA sequencing data. Genome Biol 16, 278. 10.1186/s13059-015-0844-5. [PubMed: 26653891]
33. Lehallier B., Gate D., Schaum N., Nanasi T., Lee SE., Yousef H., Moran Losada P., Berdnik D., Keller A., Verghese J., et al. . (2019). Undulating changes in human plasma proteome profiles across the lifespan. Nat Med 25, 1843–1850. 10.1038/s41591-019-0673-2. [PubMed: 31806903]
34. Perry DC, Lehmann M, Yokoyama JS, Karydas A, Lee JJ, Coppola G, Grinberg LT, Geschwind D, Seeley WW, Miller BL, et al. (2013). Progranulin mutations as risk factors for Alzheimer disease. JAMA Neurol 70, 774–778. 10.1001/2013.jamaneurol.393. [PubMed: 23609919]
35. Goedert M, and Spillantini MG (2006). Frontotemporal lobar degeneration through loss of progranulin function. Brain 129, 2808–2810. 10.1093/brain/awl291. [PubMed: 17071919]

36. Le Ber I, van der Zee J, Hannequin D, Gijselinck I, Campion D, Puel M, Laquerriere A, De Pooter T, Camuzat A, Van den Broeck M, et al. (2007). Progranulin null mutations in both sporadic and familial frontotemporal dementia. Hum Mutat 28, 846–855. 10.1002/humu.20520. [PubMed: 17436289]
37. Rademakers R, Baker M, Gass J, Adamson J, Huey ED, Momeni P, Spina S, Coppola G, Karydas AM, Stewart H, et al. (2007). Phenotypic variability associated with progranulin haploinsufficiency in patients with the common 1477C-->T (Arg493X) mutation: an international initiative. Lancet Neurol 6, 857–868. 10.1016/S1474-4422(07)70221-1. [PubMed: 17826340]
38. Tanaka Y, Chambers JK, Matsuwaki T, Yamanouchi K, and Nishihara M. (2014). Possible involvement of lysosomal dysfunction in pathological changes of the brain in aged progranulin-deficient mice. Acta Neuropathol Commun 2, 78. 10.1186/s40478-014-0078-x. [PubMed: 25022663]
39. Marschallinger J, Iram T, Zardeneta M, Lee SE, Lehallier B, Haney MS, Pluvinage JV, Mathur V, Hahn O, Morgens DW, et al. (2020). Lipid-droplet-accumulating microglia represent a dysfunctional and proinflammatory state in the aging brain. Nat Neurosci 23, 194–208. 10.1038/s41593-019-0566-1. [PubMed: 31959936]
40. Jin S, Guerrero-Juarez CF, Zhang L, Chang I, Ramos R, Kuan CH, Myung P, Plikus MV, and Nie Q. (2021). Inference and analysis of cell-cell communication using CellChat. Nat Commun 12, 1088. 10.1038/s41467-021-21246-9. [PubMed: 33597522]
41. Kim CH, Kunkel EJ, Boisvert J, Johnston B, Campbell JJ, Genovese MC, Greenberg HB, and Butcher EC (2001). Bonzo/CXCR6 expression defines type 1-polarized T-cell subsets with extralymphoid tissue homing potential. J Clin Invest 107, 595–601. 10.1172/JCI11902. [PubMed: 11238560]
42. Sariyar M, and Borg A. (2010). The RecordLinkage Package: Detecting Errors in Data. R J. 2, 61.
43. Hao Y, Hao S, Andersen-Nissen E, Mauck WM 3rd, Zheng S, Butler A, Lee MJ, Wilk AJ, Darby C, Zager M, et al. (2021). Integrated analysis of multimodal single-cell data. Cell 184, 3573–3587 e3529. 10.1016/j.cell.2021.04.048. [PubMed: 34062119]
44. Preische O., Schultz SA., Ape A., Kuhle J., Kaeser SA., Barro C., Graber S., Kuder-Buletta E., LaFougere C., Laske C., et al. . (2019). Serum neurofilament dynamics predicts neurodegeneration and clinical progression in presymptomatic Alzheimer's disease. Nat Med 25, 277–283. 10.1038/s41591-018-0304-3. [PubMed: 30664784]
45. Zhang Y, Sloan SA, Clarke LE, Caneda C, Plaza CA, Blumenthal PD, Vogel H, Steinberg GK, Edwards MS, Li G, et al. (2016). Purification and Characterization of Progenitor and Mature Human Astrocytes Reveals Transcriptional and Functional Differences with Mouse. Neuron 89, 37–53. 10.1016/j.neuron.2015.11.013. [PubMed: 26687838]
46. Gosselin D, Skola D, Coufal NG, Holtman IR, Schlachetzki JCM, Sajti E, Jaeger BN, O'Connor C, Fitzpatrick C, Pasillas MP, et al. (2017). An environment-dependent transcriptional network specifies human microglia identity. Science 356. 10.1126/science.aal3222.
47. Webster JA, Gibbs JR, Clarke J, Ray M, Zhang W, Holmans P, Rohrer K, Zhao A, Marlowe L, Kaleem M, et al. (2009). Genetic control of human brain transcript expression in Alzheimer disease. Am J Hum Genet 84, 445–458. 10.1016/j.ajhg.2009.03.011. [PubMed: 19361613]
48. Jansen IE, Savage JE, Watanabe K, Bryois J, Williams DM, Steinberg S, Sealock J, Karlsson IK, Hagg S, Athanasiu L, et al. (2019). Genome-wide meta-analysis identifies new loci and functional pathways influencing Alzheimer's disease risk. Nat Genet 51, 404–413. 10.1038/s41588-018-0311-9. [PubMed: 30617256]
49. Kunkle BW, Grenier-Boley B, Sims R, Bis JC, Damotte V, Naj AC, Boland A, Vronskaya M, van der Lee SJ, Amlie-Wolf A, et al. (2019). Genetic meta-analysis of diagnosed Alzheimer's disease identifies new risk loci and implicates Abeta, tau, immunity and lipid processing. Nat Genet 51, 414–430. 10.1038/s41588-019-0358-2. [PubMed: 30820047]
50. Yang AC, Vest RT, Kern F, Lee DP, Agam M, Maat CA, Losada PM, Chen MB, Schaum N, Khoury N, et al. (2022). A human brain vascular atlas reveals diverse mediators of Alzheimer's risk. Nature 603, 885–892. 10.1038/s41586-021-04369-3. [PubMed: 35165441]
51. Mahley RW (1988). Apolipoprotein E: cholesterol transport protein with expanding role in cell biology. Science 240, 622–630. 10.1126/science.3283935. [PubMed: 3283935]

52. Shimaoka T, Kume N, Minami M, Hayashida K, Kataoka H, Kita T, and Yonehara S. (2000). Molecular cloning of a novel scavenger receptor for oxidized low density lipoprotein, SR-PSOX, on macrophages. J Biol Chem 275, 40663–40666. 10.1074/jbc.C000761200. [PubMed: 11060282]

53. Rosen SF., Soung AL., Yang W., Ai S., Kanmogne M., Dave VA., Artyomov M., Magee JA., and Klein RS. (2022). Single-cell RNA transcriptome analysis of CNS immune cells reveals CXCL16/CXCR6 as maintenance factors for tissue-resident T cells that drive synapse elimination. Genome Med 14, 108. 10.1186/s13073-022-01111-0. [PubMed: 36153630]

54. Trelle AN, Carr VA, Guerin SA, Thieu MK, Jayakumar M, Guo W, Nadiadwala A, Corso NK, Hunt MP, Litovsky CP, et al. (2020). Hippocampal and cortical mechanisms at retrieval explain variability in episodic remembering in older adults. Elife 9. 10.7554/eLife.55335.

55. Trelle AN, Carr VA, Wilson EN, Swarovski MS, Hunt MP, Toueg TN, Tran TT, Channappa D, Corso NK, Thieu MK, et al. (2021). Association of CSF Biomarkers With Hippocampal-Dependent Memory in Preclinical Alzheimer Disease. Neurology 96, e1470–e1481. 10.1212/WNL.0000000000011477. [PubMed: 33408146]

56. McGinnis CS, Murrow LM, and Gartner ZJ (2019). DoubletFinder: Doublet Detection in Single-Cell RNA Sequencing Data Using Artificial Nearest Neighbors. Cell Syst 8, 329–337 e324. 10.1016/j.cels.2019.03.003. [PubMed: 30954475]

Highlights

- Monocytes upregulate lipid processing genes with age in cognitively normal CSF
- Monocyte lipid processing genes are dysregulated in cognitively impaired CSF
- Monocytes signal to clonal $CD8^+$ T cells via CXCL16-CXCR6 in cognitively impaired CSF
- CXCL16 is increased in cognitively impaired CSF and relates to neurodegeneration

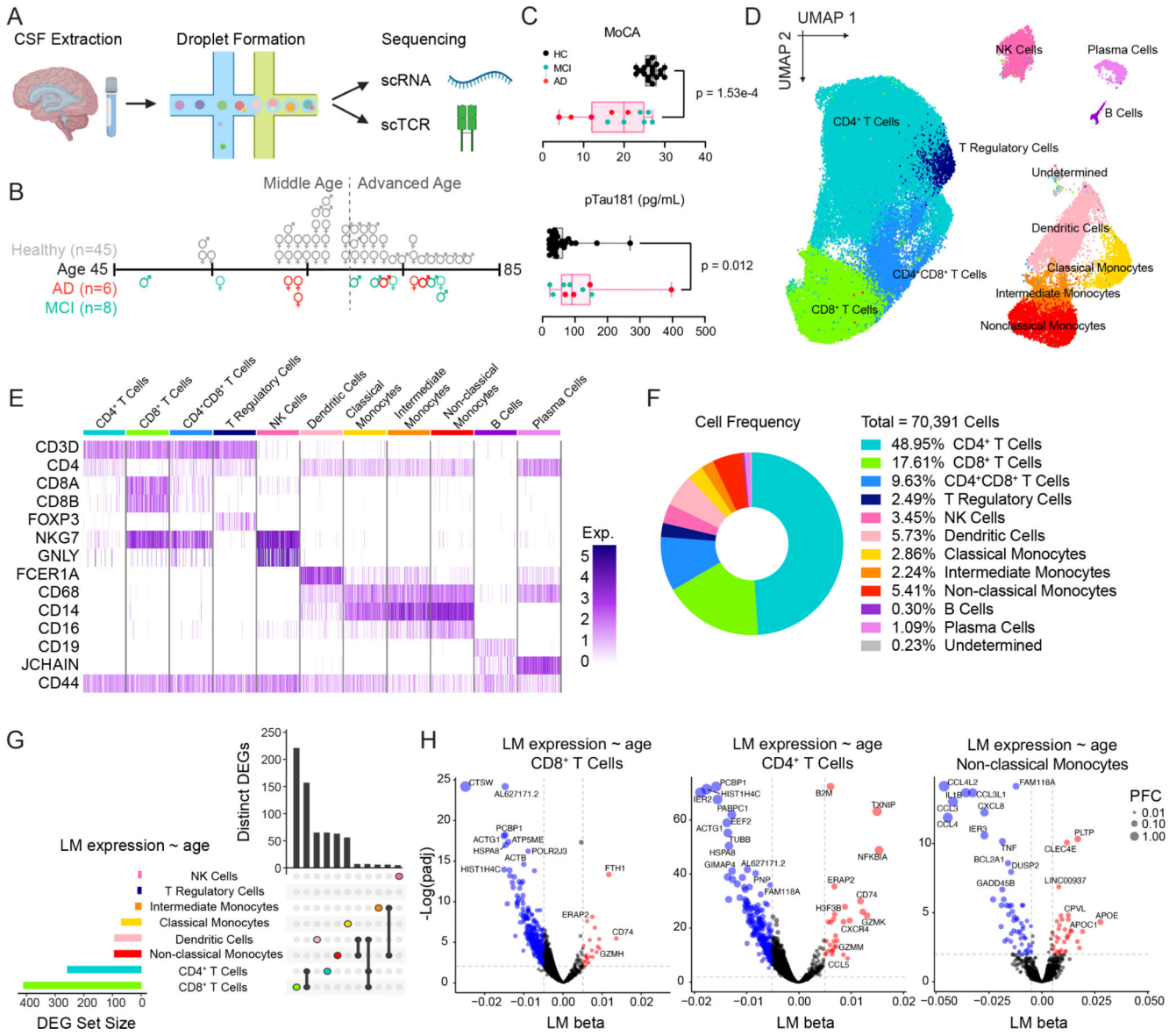

Figure 1. Study design and CSF immune cell gene expression changes by linear modeling.

A) Schematic depicting study design. CSF was isolated by lumbar puncture from living individuals. Single cells were loaded into droplets, then libraries were amplified for whole transcriptome or targeted TCR sequencing. B) Study demographics indicating age and sex of each individual. C) MoCA cognitive scores and pTau181 levels in control versus cognitively impaired subjects. Mean ± s.e.m.; Mann Whitney U test. D) UMAP plot showing clusters of CSF immune cells. E) Heatmap of marker genes utilized to annotate cell clusters. F) Donut plot indicating the distribution of CSF immune cell types. G) UpSet plot showing the number of DEGs per CSF immune cell cluster. H) Volcano plots depicting DEGs of the most altered clusters by linear modeling (LM). See also Figure S1 and Table S1.

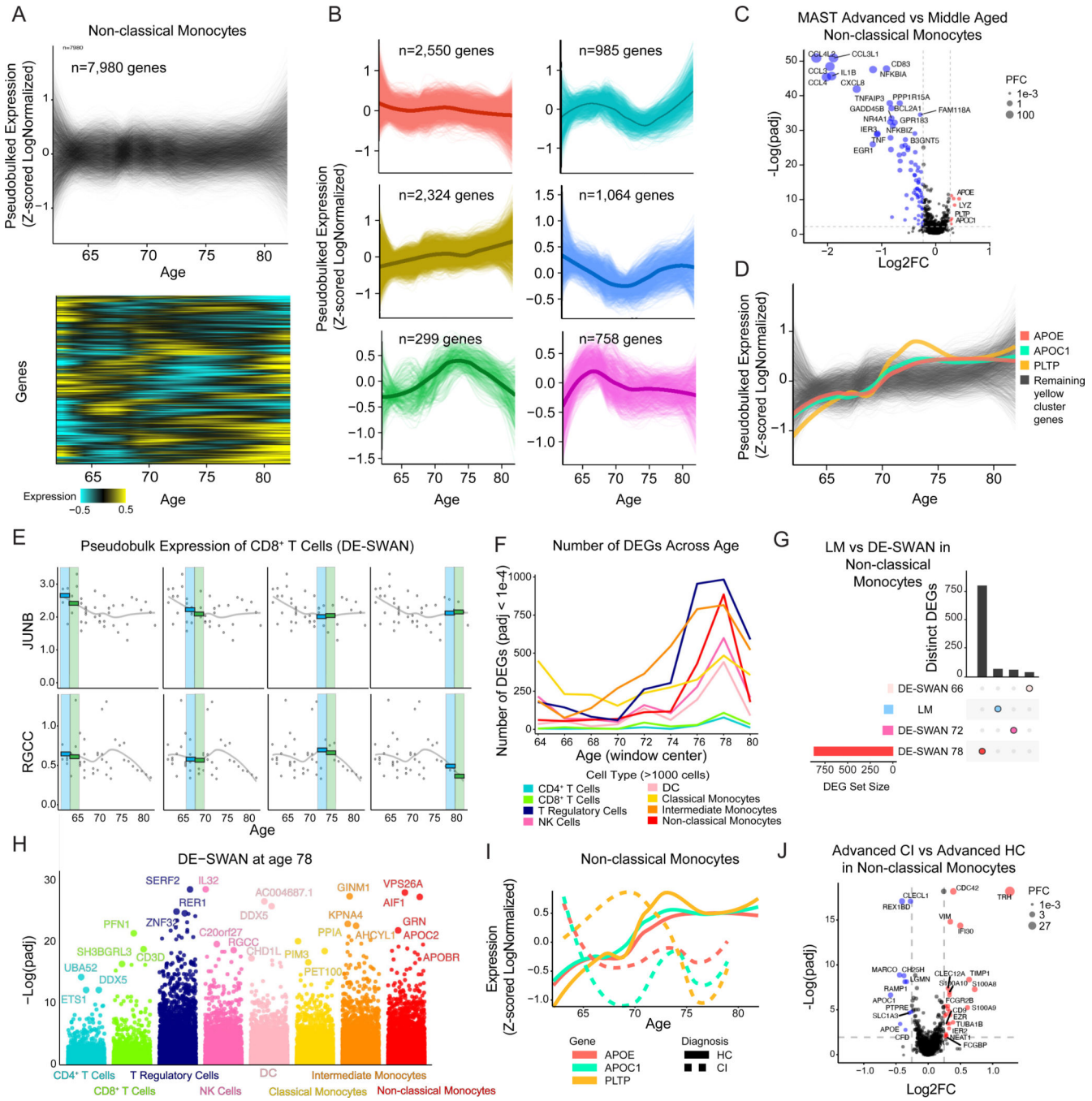

Figure 2. Upregulated lipid processing gene expression in activated CSF monocytes with age.

A) LOESS trajectories (upper) and a corresponding heat map (lower) demonstrating wave-like expression patterns of activated monocytes with age. B) Sets of genes ordered by hierarchical clustering and displayed using LOESS trajectories display distinct wave-like patterns with age. C) Volcano plot from MAST differential expression analysis showing downregulation of cytokine genes and upregulation of lipid processing genes. D) LOESS trajectories of *APOE*, *APOC1* and *PLTP* expression in activated CSF monocytes with age. E) Representative genes *JUNB* and *RGCC* displaying distinct non-linear changes with age.

DE-SWAN was used to measure the age at which most differential expression occurs. F) Results of DE-SWAN analysis indicating a consistent dysregulation of CSF immune cell types at age 78. G) UpSet plot comparing the number of DEGs for activated CSF monocytes from DE-SWAN and linear modeling. H) Manhattan plot indicating genes that were differentially expressed by each cluster at age 78. I) LOESS trajectories of lipid processing genes comparing healthy controls to cognitively impaired subjects. J) Volcano plot showing reduction of lipid processing genes *APOE* and *APOC1* comparing only advanced aged subjects. See also Figure S2–3 and Table S2–5.

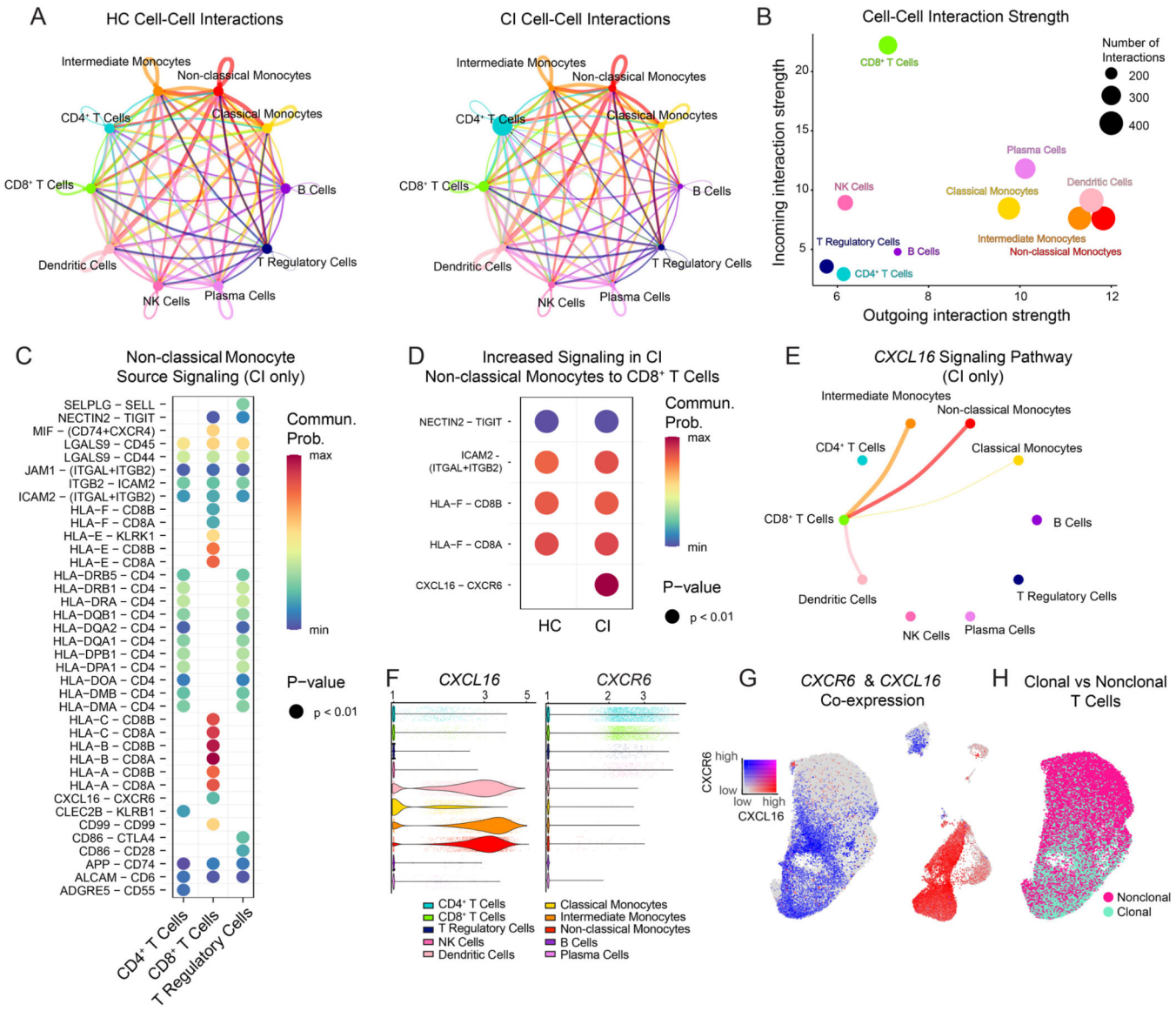

Figure 3. Cell-cell communication algorithm indicates non-classical monocytes communicate with CD8$^+$ T cells via CXCL16-CXCR6 signaling in cognitive impaired CSF.

A) Circle plots of signaling networks of healthy and cognitively impaired CSF immune systems. B) Cell-cell interaction strengths plotted for all cell types indicating incoming and outgoing interactions. C) Dot plot indicating signaling molecules between non-classical monocytes and T cells in cognitively impaired CSF. D) CXCL16-CXCR6 signaling between non-classical monocytes and CD8$^+$ T cells is unique to cognitively impaired CSF. E) The signaling network for CXCL16-CXCL6 indicates activated monocytes as the primary source of CXCL16 for CXCR6 on CD8$^+$ T cells. F) Violin plots indicating which cell types express CXCR6 and CXCL16 in the CSF. G) UMAP showing expression of CXCR6 by T cells and CXCL16 by myeloid cells. H) Distribution of clonal and nonclonal CSF T cells.

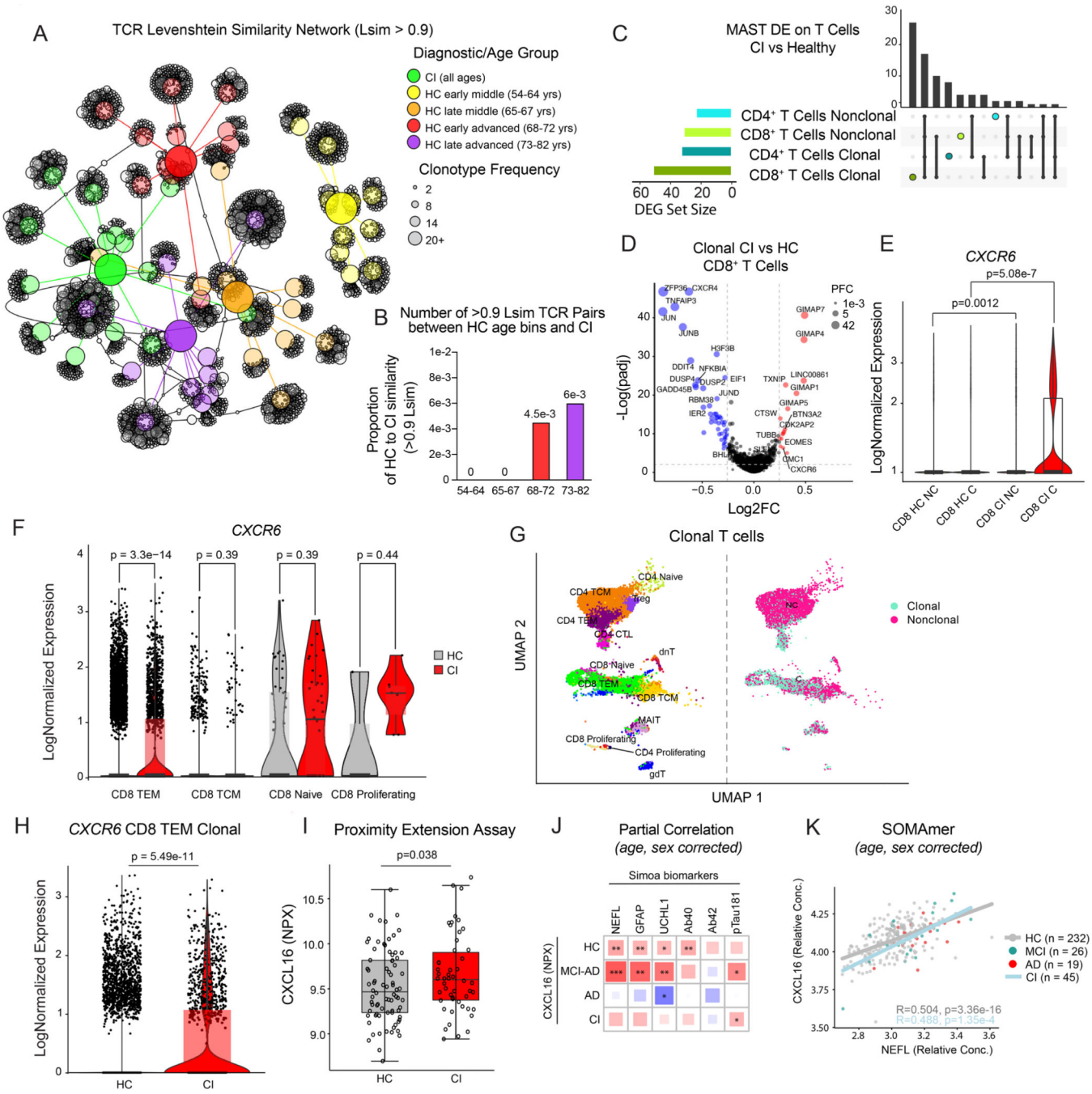

Figure 4. Clonally expanded T cell disruption in CSF of patients with cognitive impairment.

A) TCR networking plot depicting Levenshtein similarities > 0.9 for all clonal CSF TCRs. Healthy, cognitively normal patients were binned into equal sized groups. B) Quantification of the proportion of TCRs for each age group that had Levenshtein similarity > 0.9. C) UpSet plot showing that clonally expanded $CD4^+$ and $CD8^+$ T cells have more DEGs that nonclonal T cells. D) Volcano plots showing DEGs of clonal vs. nonclonal $CD8^+$ T cells between cognitively impaired and healthy CSF. E) Quantification of average single cell expression of clonal and nonclonal $CD8^+$ T cells from cognitively impaired and healthy

CSF. P-values are from MAST differential expression. F) Single cell quantification of CXCR6 expression by $CD8^+$ T cell subtypes showing increased expression among $CD8^+$ T_{EM} cells. G) UMAP showing distribution of T cell subtypes and clonality using supervised clustering. H) Single cell quantification of *CXCR6* expression in clonal $CD8^+$ T_{EM} cells showing higher expression among cognitively impaired subjects. I) PEA assay measurement of CXCL16 protein showing higher levels in cognitively impaired subjects. J) Correlations of CXCL16 with CSF biomarkers. K) Correlations between CSF CXCL16 and NEFL using SOMAmer measurements. See also Figure S4–6 and Table S4–5.

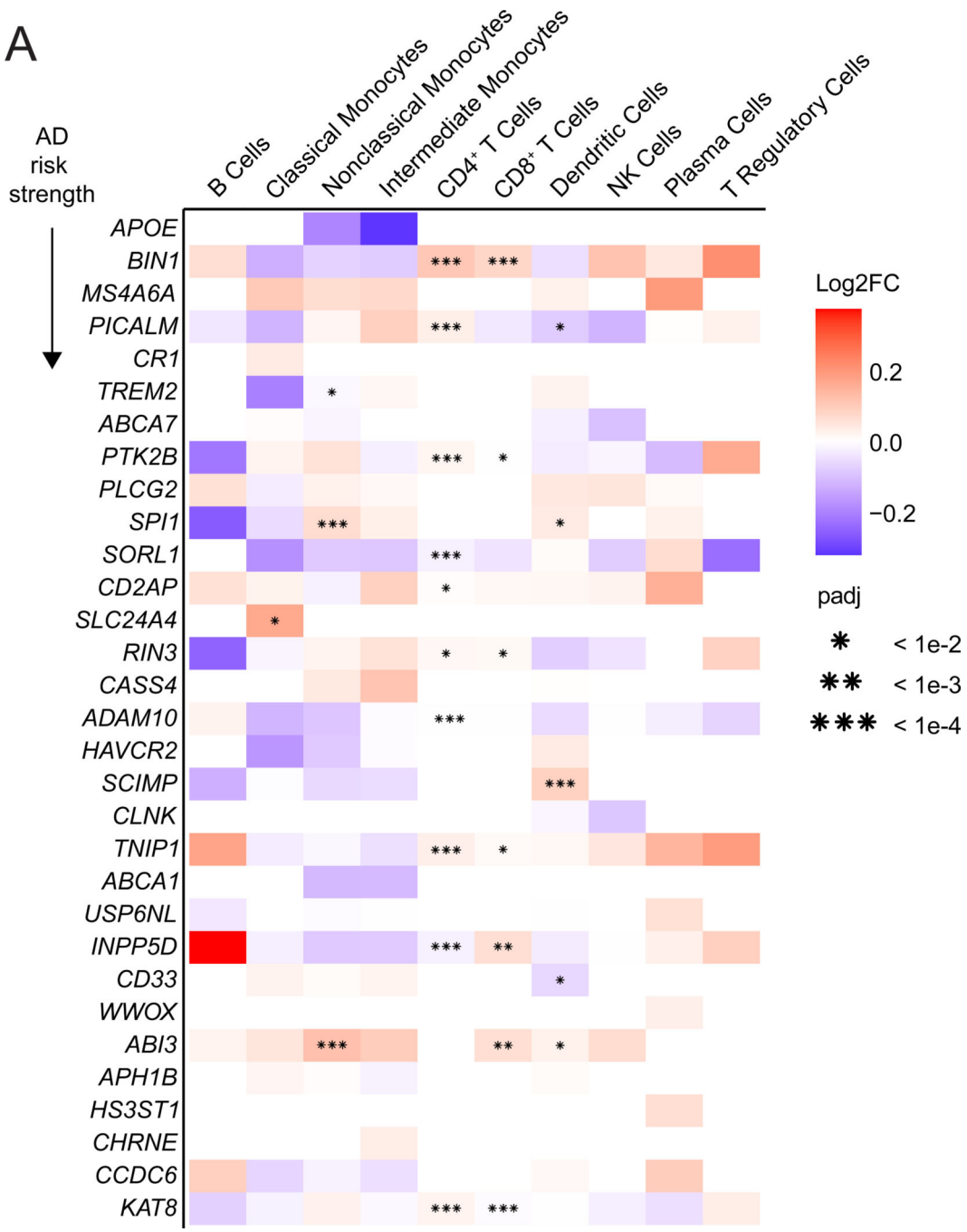

Figure 5. Differential expression of the top 45 AD GWAS genes across all major CSF immune cell types.

Asterisks denote the most highly altered genes by adjusted p-value. Note that T cells differentially express numerous AD risk genes in CI CSF. See also Figure S7.

Table 1.

Demographics and biomarker data of study subjects.

		HC	CI	P
Demographics				
Cognitive Impairment, n (%)	HC	45 (100.0%)	0 (0.0%)	<0.001
	MCI	0 (0.0%)	8 (57.1%)	
	AD	0 (0.0%)	6 (42.9%)	
Sex, n (%)	Female	27 (60.0%)	7 (50.0%)	0.725
	Male	18 (40.0%)	7 (50.0%)	
Age	Median (IQR)	69.0 (65.0 to 73.0)	72.5 (64.0 to 76.8)	0.475
Race, n (%)	Asian	3 (6.7%)	1 (7.1%)	0.565
	Native Hawaiian or Other Pacific Islander	1 (2.2%)		
	White	35 (77.8%)	9 (64.3%)	
	N/A	6 (13.3%)	4 (28.6%)	
APOE Genotype		**n = 38**	**n = 10**	
	E3/E2	4 (10.5%)	1 (10.0%)	0.360
	E3/E3	16 (42.1%)	2 (20.0%)	
	E3/E4	16 (42.1%)	5 (50.0%)	
	E4/E4	2 (5.3%)	2 (20.0%)	
MoCA Score		**n = 22**	**n = 12**	
	Median (IQR)	27.0 (26.0 to 28.0)	20.5 (15.0 to 24.2)	<0.001
CDR		**n = 42**	**n = 11**	
	Median (IQR)	0.0 (0.0 to 0.0)	1.0 (1.0 to 3.2)	<0.001
CSF Biomarkers (pg/mL)		**n = 37**	**n = 10**	
pTau181	Median (IQR)	40.1 (32.9 to 61.2)	91.1 (67.2 to 141.8)	0.012
Total Tau	Median (IQR)	302.0 (265.0 to 412.3)	604.6 (453.3 to 819.7)	0.006
Aβ42	Median (IQR)	1,000.0 (811.3 to 1,231.3)	870.1 (673.8 to 1,014.8)	0.311
Aβ40	Median (IQR)	10,565.0 (8,81,6.0 to 12,383.0)	12,061.5 (9,888.0 to 13,718.5)	0.203
CSF Biomarker Ratios		**n = 37**	**n = 10**	
Aβ42/ Aβ40	Median (IQR)	0.115 (0.078 to 0.126)	0.073 (0.063 to 0.115)	0.264
Aβ42/Total Tau	Median (IQR)	3.900 (2.033 to 4.577)	1.247 (1.036 to 2.611)	0.015

Key resources table

REAGENT or RESOURCE	SOURCE	IDENTIFIER
Antibodies		
Rat monoclonal anti-CD3	Abcam	ab11089
Rabbit monoclonal anti-CXCR6	Abcam	ab273116
Mouse monoclonal anti-CXCL16	Thermo Fisher	MA5–27845
Rabbit monoclonal anti-amyloid-β	Cell Signalling	8243
Goat polyclonal anti-Iba1	Abcam	ab48004
Biological samples		
Adult CSF	Stanford Aging and Memory Study (SAMS)	n/a
Adult CSF	Stanford University Alzheimer's Disease Research Center (ADRC)	n/a
Adult CSF	University of California at San Francisco ADRC	n/a
Adult CSF	University of California at San Diego ADRC	n/a
Critical commercial assays		
10x Genomics Chromium Next GEM Single Cell 5' v2 with immune profiling kit	10xGenomics	PN-1000263
Deposited data		
Raw and processed data	This study	GEO: GEO200164
Code for analysis	This study	Github: https://github.com/gatelabnw/csf_aging
ShinyCell app for interactive data analysis	This study	ShinyApps:gatelabnu.shinyapps.io/csf_aging
Software and algorithms		
Cellranger v6.0.0	10x Genomics	https://support.10xgenomics.com/single-cell-gene-expression/software/pipelines/latest/what-is-cell-ranger
SoupX v1.5.2	Young and Behjati[18]	https://github.com/constantAmateur/SoupX
DoubletFinder v2.0.3	McGinnis et al.[56]	https://github.com/chris-mcginnis-ucsf/DoubletFinder
Seurat v4.1.0	Hao et al.[42]	https://satijalab.org/seurat/
DEswan v0.0.0.9001	Lehallier et al.[33]	https://github.com/lehallib/DEswan
CellChat v1.4.0	Jin et al.[40]	http://www.cellchat.org
RecordLinkage v0.4–12.3	Sariyar and Borg[42]	https://cran.r-project.org/web/packages/RecordLinkage/index.html